[2] DIMOCK, D.L., EUBANK, H.P., HINNOV, E., JOHNSON, L.C., MESERVEY, E.B., Nucl. Fusion **13** (1973) 271.
[3] HUTCHINSON, I.H., MORTON, A.H., Nucl. Fusion **16** (1976) 447.
[4] MIRNOV, S.V., SEMENOV, I.B., Sov. J. Plasma Phys. **4** (1978) 27.
[5] GRANETZ, R.S., HUTCHINSON, I.H., OVERSKEI, D.O., Nucl. Fusion **19** (1979) 1587.
[6] HAWRYLUK, R.J., BRETZ, N., DIMOCK, D., HINNOV, E., JOHNSON, D., MONTICELLO, D., McCUNE, D., SUCKEWER, S., Current Penetration in the PLT Tokamak, Plasma Physics Lab., Princeton Univ., NJ, Rep. PPPL-1572 (1980).
[7] TOI, K., SAKURAI, K., TANAHASHI, S., YASUE, S., Nucl. Fusion **22** (1982) 465.
[8] KARGER, K., KLUEBER, O., NIEDERMEYER, H., SCHUELLER, F.C., THOMAS, P.R., in Controlled Fusion and Plasma Physics (Proc. 11th Europ. Conf. Aachen, 1983), Vol. 1, ECA, Linnich (1983) 63.
[9] MEYERHOFER, D.D., GOLDSTON, R.J., KAITA, R., CAVALLO, A., GREK, B., JOHNSON, D., McCUNE, D.C., McGUIRE, K., WHITE, R.B., Nucl. Fusion **25** (1985) 321.
[10] BELL, M.G., CHEETHAM, A.D., HAMBERGER, S.M., HOGG, G.R., HOLLIS, M.J., HOW, J.A., KUWAHARA, H., MORTON, A.H., Aust. J. Phys. **37** (1984) 137.
[11] CHEETHAM, A.D., HAMBERGER, S.M., HOW, J.A., KUWAHARA, H., MORTON, A.H., SHARP, L.E., Aust. J. Phys. **39** (1986) 35.
[12] CHEETHAM, A.D., HAMBERGER, S.M., HOGG, G.R., HOW, J.A., KUWAHARA, H., MORTON, A.H., SHARP, L.E., VANCE, C.F., in Controlled Fusion and Plasma Physics (Proc. 11th Europ. Conf. Aachen, 1983), Vol. 1, ECA, Linnich (1983) 81.
[13] WESSON, J.A., Nucl. Fusion **18** (1978) 87.
[14] CROSS, R.C., KOCHANSKI, T.P., SNIPES, J.A., KIM, S.B., POWERS, E.J., Bull. Am. Phys. Soc. **29** (1984) 1395.
CROSS, R.C., private communication, 1985.

(Manuscript received 5 November 1985
Final manuscript received 24 April 1986)

DEPENDENCE OF RESISTIVE LOADING ON ANTENNA ORIENTATION FOR ICRF WAVES IN A TOKAMAK

S. SHINOHARA, O. NAITO, K. MIYAMOTO
(Department of Physics, Faculty of Science, University of Tokyo, Bunkyo-ku, Tokyo, Japan)

ABSTRACT. The parameter dependence of antenna loading resistance for ICRF waves using a T-shaped rotatable antenna is investigated in the TNT-A tokamak. When the antenna current is parallel to the toroidal field, the loading resistance increases with the mean plasma density, but depends weakly on the toroidal field, the ratio of hydrogen to deuterium concentrations and the type of the Faraday shield. Similar results with a lower value of the loading resistance are obtained in the case where the antenna current is perpendicular to the toroidal field, using the same rotatable antenna. With the antenna current parallel to the toroidal field, the loading resistance for a low parallel refractive index n_z is larger than that for high n_z.

1. INTRODUCTION

Radio frequency heating near the ion cyclotron range of frequency (ICRF) [1] is one of the most attractive means of supplementary heating in tokamaks. Heating of ions by the fast magnetosonic wave has been studied successfully in many tokamaks [2–5]. Recently, plasma heating by the ion Bernstein wave (IBW) [6], which has the capability of waveguide operation, at the ion cyclotron harmonic frequency has been anticipated as a promising method. Although mode conversion from the fast magnetosonic wave to the ion Bernstein wave has been studied in several tokamaks [7–11], directly launched ion Bernstein wave experiments are few: excitation, propagation and heating by this wave were studied in ACT-1, a low temperature toroidal device [12, 13]. In the JIPPT-II-U tokamak, efficient ion heating was observed at the third harmonic frequency of the $^4He^{2+}$ minority ion [5, 14]. Experimental measurements, with the IBW, of the dependence of antenna loading resistance, which is related to the efficiency of energy transfer from the exciting system, are not yet sufficient, and the difference in loading resistance between ion Bernstein and fast magnetosonic waves has not been studied extensively. Therefore, experimental studies of these subjects are very important for the design of a heating system.

Up to now, the excitation of a fast magnetosonic wave by an antenna current perpendicular to the toroidal field (E_θ antenna) and of an ion Bernstein wave by a current parallel to the field (E_z antenna)

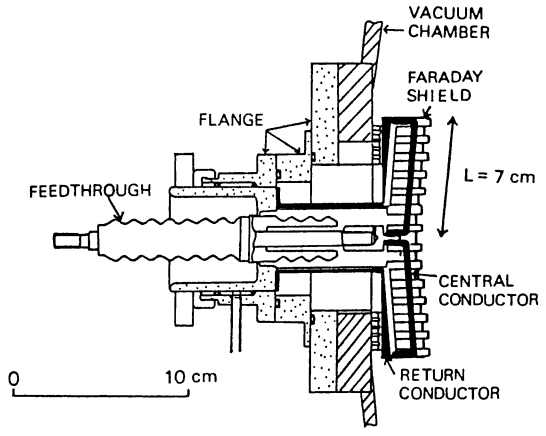

FIG. 1. Cross-sectional view of T-shaped ICRF antenna. There are two central copper conductors (7 cm long each) with rectangular cross-section, 0.3 cm thick and 1.6 cm wide; other parts are made of stainless steel of 0.1 cm thickness. Faraday shield is used to reduce excited electric field perpendicular to antenna current. This antenna is used as E_z as well as E_θ antenna since feedthrough part is rotatable.

has been tried. In fact, however, both waves can be excited for either antenna orientation; in view of the alignment of the Faraday shield, the ratio of power coupling from one wave to another is less than several per cent [15]. Significant coupling to the ion Bernstein wave can be found due to parametric excitation [16] or direct conversion [17] of the fast magnetosonic wave.

In any case, a study of the antenna coupling, as a function of changing the antenna orientation, is very important, and there are only few results on antenna loading using an E_z antenna. In this paper, the dependence of the loading resistance as measured by ICRF waves is reported for the TNT-A tokamak [18, 19] using a T-shaped rotatable antenna. In Section 2, the experimental setup is described. The parameter dependence (plasma density, toroidal field, ratio of hydrogen to deuterium concentrations, type of Faraday shield, and parallel refractive index) of the loading resistance is investigated by using the E_z antenna, and comparisons with the results using the E_θ antenna are described in Section 3. Conclusions are presented in Section 4.

2. EXPERIMENTAL SETUP

Typical experimental parameters in the non-circular tokamak TNT-A are as follows: major radius R = 40 cm, minor radius a = 9 cm, elongation ratio κ = 1.2, plasma current I_p = 3 – 5 kA, loop voltage V_ℓ = 5 – 9 V, mean plasma density $\bar{n}_e = (0.4 - 1.2) \times 10^{13}$ cm^{-3}, central electron temperature $T_e(0) \approx 30$ eV, discharge duration time ~20 ms, and ratio of radiated power, by bolometer, to Ohmic power = 0.7 – 0.95.

A cross-sectional view of the T-shaped antenna, located on the low field side of the torus, is shown in Fig. 1. There are two central copper conductors (each 7 cm long) with rectangular cross-section, 0.3 cm thick and 1.6 cm wide; other parts are made of stainless steel of 0.1 cm thickness. A Faraday shield is used to reduce the excited electric field perpendicular to the antenna current. Two types of Faraday shield screens are provided: each strip of the inner screen is 0.4 cm wide and each gap has a width of 0.4 cm. The outer screen has strip of 0.4 cm width, and each gap has a width of 0.6 cm. Both return conductors are connected to the vacuum chamber. The antenna is located at nearly the same radial position as the fixed limiter, a = 9 cm, and is 180° toroidally away from this limiter.

The antenna current flows from the feedthrough to the two central conductors, which have opposing current directions. We say 'half' and 'full' when one and two central conductors are used, respectively. As this antenna is rotatable at the feedthrough part, both electric fields E_z and E_θ can be excited when the antenna current is parallel or perpendicular to the toroidal field, respectively.

The frequency f of the generator is 5.6 MHz, the pulse width is up to 10 ms, and a typical RF power in these experiments is 10 kW.

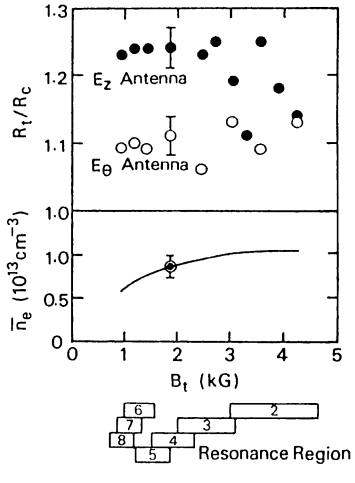

FIG. 2. Dependence of normalized loading resistance R_t/R_c on toroidal field obtained by the same rotatable antenna for excitation of E_z and E_θ. One of central conductors and single screens with $n_H/(n_H + n_D) = 0.1$ (n_H: hydrogen density, n_D: deuterium density) is used. Mean plasma density and resonance region of deuteron cyclotron harmonic in the plasma are also shown.

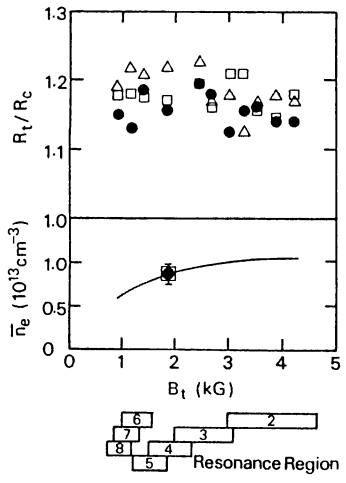

FIG.3. Dependence of normalized loading resistance R_t/R_c on toroidal field for E_z antenna direction with one of central conductors and single screens. Here, triangles, squares and closed circles mean $n_H/(n_H + n_D) = 0.9$, 0.5 and 0.1, respectively. Mean plasma density and resonance region of deuteron cyclotron harmonic in the plasma are also shown.

3. EXPERIMENTAL RESULTS OF ANTENNA LOADING

Antenna loading by the E_z antenna is investigated experimentally by using one of the central conductors and single (inner) screens. First, the dependence of the loading resistance on the toroidal field is studied, as is shown in Fig. 2 ($n_H/(n_H + n_D) = 0.1$, where n_H and n_D are the hydrogen and the deuterium density, respectively). Here, the loading resistance R is defined as $R = P_{inp}/I^2$, where P_{inp} is the input power from the generator and I is the antenna current. (When both central conductors are used, we take the sum of both antenna currents as the value of I.) We denote the vacuum loading resistance by R_c ($\sim 0.3\ \Omega$) and the total loading resistance by R_t in the presence of the plasma. In the case of the E_z antenna, $R_t/R_c \approx 1.2$, and this value is higher than that with the E_θ antenna, which is ~ 1.1. Although all parts of the E_z antenna are at the same distance with respect to the plasma, the antenna tips are farther away from the plasma than the feeders, by ~ 1.5 cm, with the E_θ antenna. The decrease in loading resistance due to this effect with the E_θ antenna is estimated to be at most 10–15% of the previous experimental results using a movable limiter in order to change the antenna-plasma distance [20], and at most 20% of the calculated value [20] using a slab model [21]. Therefore, it can be said that the coupling obtained experimentally by the E_θ antenna is somewhat weaker than that with the E_z antenna.

The antenna loading as obtained with the E_θ antenna has nearly the same value (within a factor of two) as the results computed from the code [21]. The previous experimental results for the direction of the E_θ antenna also showed good correspondence with the results of this calculation [20]. As to the E_z antenna case, there are a few theoretical models that can be applied to the present experiments. The following estimates have been carried out by using simple models: according to Refs [23, 24], the loading resistance is very sensitive to the edge plasma density, but the computed results show that the experimental values lie in the region of estimated values. The values of loading resistance obtained from Ref. [25] are also of the same magnitude as the experimental values.

From Fig. 2, we see that the loading resistance is weakly dependent on the toroidal field. By changing the ratio of the hydrogen to deuterium concentration, no appreciable change in the loading resistance is observed using E_z antenna orientation, as is shown in Fig. 3. The weak dependence of the antenna loading on the toroidal field and the ratio of hydrogen to deuterium densities indicates that collisions between neutrals and charged particles in the TNT-A plasma cannot be neglected in the calculation using the same code as in Ref. [21] and also indicates that part of the RF power is directly absorbed in the peripheral plasma region [22]. The dependence obtained with the E_θ antenna is consistent with previous experimental results [20].

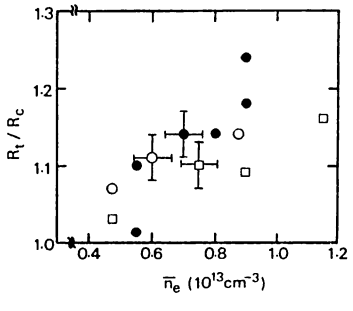

FIG.4. Relation between normalized loading resistance R_t/R_c and mean plasma density with $n_H/(n_H + n_D) = 0.1$, if one of central conductors and single screens are used. Closed circles, open circles and squares show E_z antenna orientation case at $\omega = 4\omega_D$, and E_θ antenna at $\omega = 4\omega_D$ and $\omega = 2\omega_D$, respectively (ω_D: deuteron cyclotron frequency near plasma centre).

Next, the relation between the loading resistance and the mean plasma density is investigated. Figure 4 shows that the loading resistance increases with the mean plasma density for both E_z and E_θ directions. In both orientations, a mean plasma density above $\sim 10^{13}$ cm^{-3} is favourable from the viewpoint of higher resistance of antenna loading. There is a tendency for the dependence of the loading resistance on the mean plasma density to be stronger for E_z antenna than for E_θ antenna direction.

The fact that the antenna loading using the E_z antenna orientation increases with higher plasma density agrees well with the results of the calculation and experiments done in ACT-1 for the case of $\omega \approx 2\omega_D$ (ω_D is deuteron cyclotron frequency) [23]. However, other theories on the ion Bernstein wave are inconsistent with the present experimental results with the E_z antenna direction: the loading resistance decreases with n_{edge} (n_{edge} is the plasma density at the antenna surface) [24] and is nearly independent of the plasma density in the range of $\omega \approx 2\omega_D$ [25] in TNT-A parameters. The obtained dependence on the mean plasma density with the E_θ antenna direction is consistent with previous experimental results [20] and the computed results using the slab model [21, 26].

With increasing input power, the loading resistance decreases for both orientations. The reason for this feature is unclear, but the change in the plasma parameters near the antenna may affect the loading resistance [20]. With the increase in input power, an increase in the electron temperature and a decrease in the plasma density near the antenna are observed by Langmuir probe measurements.

Preliminary experiments on the excitation of a unidirectional travelling wave in the toroidal direction by the E_z antenna orientation have been carried out, although the fraction of the directivity is not so good. (The power coupling to one direction is estimated to be ~ 2.5 times of that to another direction.) In this case, two central conductors with the capacitors are used to produce a phase difference between the currents of the two central conductors. The capacitors (0.06 μF) are connected between the top of the feedthrough (vacuum side) and high voltage side of one of the central conductors. Under certain conditions with low plasma density ($\lesssim 10^{12}$ cm^{-3}) and low plasma current ($\lesssim 1$ kA), the normalized loading resistance R_t/R_c becomes ≈ 1.1, and the plasma current and the soft X-ray emissivity above 150 eV increase by a factor of $\lesssim 2$. The cause of these phenomena is not clear, but the plasma parameters near the antenna seem to play an important role.

TABLE I. SUMMARY OF NORMALIZED LOADING RESISTANCE R_t/R_c FOR VARIOUS CONFIGURATIONS BY E_z AND E_θ ANTENNAS (R_c: VACUUM LOADING RESISTANCE, R_t: TOTAL LOADING RESISTANCE).
"Half" and "full" refer to the use of one and two (one pair) central conductors. Use of two types of screens (inner and outer screens) of the Faraday shield is designated by "double", the inner screens by "single" and the inner screens with a gap of 1.4 cm width by "single (sparse)".

Excitation	Screen / Conductor	Double	Single	Single (sparse)
E_z Antenna	Full	~1	~1	~1
	Half		~1.2	≲1.2
E_θ Antenna	Full		~1	
	Half		~1.1	

Finally, experimental results on the loading resistance for various antenna configurations are summarized, as is shown in Table I. From this table, the loading resistance depends weakly on the type of Faraday shield for the E_z antenna direction. This resistance by E_z antenna direction is a little larger than that by E_θ antenna direction by the use of one of the central conductors (half). When the pair of central conductors (full) is used, the total loading resistance R_t is almost the same as the vacuum loading resistance R_c for both E_z and E_θ antenna directions.

In comparing one and two loop excitations (half and full), the antenna size is different for the use of one or two central conductors, but the total change of the inductance (from antenna to feedthrough) and the change of R_c are small ($<10\%$), experimentally. From the previous experiments using the E_θ antenna direction in TNT-A [20] and other machines, we see that the antenna loading increases with the size of the antenna for a fixed antenna spectrum. Therefore, if we can assume that the antenna loading does not depend on the antenna current spectrum, this loading is expected to increase when two central conductors are used instead of one. This is different from the present experimental result that the antenna loading for one conductor is higher than that for two conductors; so, it shows a dependence on the antenna current spectrum.

In the E_θ antenna direction case with the pair of central conductors (full), the antenna spectra between the two conductors are the same except for opposite signs obtained from the calculation. It is therefore expected in TNT-A that each of the two central conductors lowers the intensity of the excited antenna spectrum of the other one, which leads to the low value of the experimental antenna loading.

In the E_z antenna direction case, the antenna current spectra are $\propto \sin(\phi/2)/(\phi/2)$ (long wavelength mode, peaked at $n_z = 0$) and $\propto(1 - \cos\phi)/\phi$ (short wavelength mode, peaked at $n_z = 280$), obtained by using one (half) and two (full) central conductors, respectively. Here, $\phi = k_z$ (parallel wavenumber) $\times$ L (antenna length of one central conductor (see Fig. 1)). From these formulae, the fraction of the antenna spectrum at small k_z is larger for the use of one central conductor than it is for the use of two. This indicates that the antenna loading at high parallel refractive index n_z is lower than that at low n_z using the E_z antenna direction from the experiments and the antenna current spectrum.

From the calculation for TNT-A parameters, using Ref. [25], the antenna loading using the E_z orientation is zero at $n_z = 0$, peaked at $n_z = 80$, and then decreases with n_z. Considering the antenna current spectrum excited in this E_z antenna, we expect from this calculation that the antenna loading is higher for the use of one central conductor than that for two conductors, which is consistent with the present experimental results. The results of the calculation and experiments in ACT-1 [23] also support this conclusion.

4. CONCLUSIONS

The parameter dependence of the antenna loading resistance for the E_z antenna orientation (f = 5.6 MHz and $P_{inp} \approx 10$ kW) has been investigated in the TNT-A tokamak. The loading resistance increases with the mean plasma density ($0.4 \times 10^{13} < \bar{n}_e < 1.2 \times 10^{13}$ cm^{-3}), but depends weakly on the toroidal field (i.e. $2\omega_D \lesssim \omega \lesssim 8\omega_D$), the ratio of hydrogen to deuterium concentrations ($n_H/(n_H+n_D) = 0.1$, 0.5 and 0.9) and the type of Faraday shield (double, single and single (sparse)). Similar results with a lower value of the loading resistance ($R_t/R_c \approx 1.1$) are obtained by the E_θ antenna direction of the same rotatable antenna.

In the case of the E_z antenna direction, the loading resistance at low parallel refractive index n_z is larger than that at high n_z. The wave heating at $2\omega_D \lesssim \omega \lesssim 3\omega_D$ by the E_z antenna and a comparison with the wave heating by the E_θ antenna are under study.

ACKNOWLEDGEMENT

This work was partly supported by a grant-in-aid for scientific research from the Japanese Ministry of Education.

REFERENCES

[1] STIX, T.H., Nucl. Fusion **15** (1975) 737.
[2] MAZZUCATO, E., BELL, M., CAVALLO, A., COHEN, S., COLESTOCK, P., et al., in Plasma Physics and Controlled Nuclear Fusion Research 1984 (Proc. 10th Int. Conf. London, 1984), Vol. 1, IAEA, Vienna (1985) 433.
[3] EQUIPE TFR, ibid., 103.
[4] MORI, M., HASEGAWA, K., HONDA, A., HOSHINO, K., ISHIBORI, I., et al.,ibid., 445.
[5] TOI, K., WATARI, T., OHKUBO, K., KAWAHATA, K., NODA, N., et al.,ibid., 523.
[6] BERNSTEIN, I.B., Phys. Rev. Lett. **109** (1958) 10.
[7] LEE, P., TAYLOR, R.J., PEEBLES, W.A., PARK, H., YU, C.X., XU, Y., LUHMANN, N.C., Jr., JIN, S.X., Phys. Rev. Lett. **49** (1982) 205.
[8] TFR GROUP, TRUC, A., GRESILLON, D., Nucl. Fusion **22** (1982) 1577.
[9] IDA, K., NAITO, M., SHINOHARA, S., MIYAMOTO, K., Nucl. Fusion **23** (1983) 1259.
[10] IDA, K., NAITO, O., OCHIAI, I., SHINOHARA, S., MIYAMOTO, K., Nucl. Fusion **24** (1984) 375.
[11] PARK, H., LUHMANN, N.C., Jr., PEEBLES, W.A., KIRKWOOD, R., Phys. Rev. Lett. **52** (1984) 1609.
[12] ONO, M., WONG, K.L., WURDEN, G.A., Phys. Fluids **26** (1983) 298.
[13] ONO, M., WURDEN, G.A., WONG, K.L., Phys. Rev. Lett. **52** (1984) 37.
[14] ONO, M., WATARI, T., ANDO, R., FUJITA, J., HIROKURA, Y., et al., Phys. Rev. Lett. **54** (1985) 2239.
[15] PURI, S., Phys. Fluids **27** (1984) 2156.
[16] SKIFF, F., ONO, M., WONG, K.L., Phys. Fluids **27** (1984) 1051.
[17] MORALES, G.J., ANTANI, S.N., FRIED, B.D., Phys. Fluids **28** (1985) 3302.
[18] TOI, K., ITOH, S., KAWAI, Y., HIRAKI, N., NAKAMURA, K., et al., in Plasma Physics and Controlled Nuclear Fusion Research 1980 (Proc. 8th Int. Conf. Brussels, 1980), Vol. 1, IAEA, Vienna (1981) 721.
[19] SHINOHARA, S., SAKUMA, K., NAGAYAMA, Y., TOYAMA, H., J. Phys. Soc. Jpn. **52** (1983) 94.

[20] SHINOHARA, S., ASAKURA, N., NAITO, M., MIYAMOTO, K., J. Phys. Soc. Jpn. 53 (1984) 1746.
[21] FUKUYAMA, A., NISHIZAWA, S., ITOH, K., ITOH, S.I., Nucl. Fusion 23 (1983) 1005.
[22] TFR GROUP, SAND, F., Nucl. Fusion 25 (1985) 1719.
[23] SKIFF, F., ONO, M., COLESTOCK, P., WONG, K.L., Phys. Fluids 28 (1985) 2453.
[24] PURI, S., Phys. Fluids 26 (1983) 164.
[25] SY, W.N.-C., AMANO, T., ANDO, R., FUKUYAMA, A., WATARI, T., Nucl. Fusion 25 (1985) 795.
[26] SHINOHARA, S., NAITO, M., MIYAMOTO, K., J. Phys. Soc. Jpn. 52 (1983) 2622.

(Manuscript received 12 August 1985
Final manuscript received 28 April 1986)

DRIFT INSTABILITY IN TOKAMAKS

A. HIROSE (Department of Physics, University of Saskatchewan, Saskatoon, Saskatchewan, Canada)

ABSTRACT. Drift waves are shown to be absolutely unstable in tokamak geometry with Landau damping on thermal electrons alone (universal instability). Toroidicity induced frequency downshift is responsible for destabilization.

The universal drift mode due to Landau damping on electrons alone (without collisional dissipation and trapped particle effects) is known to be absolutely stable in a sheared magnetic field [1, 2]. Subsequent studies [3] in the tokamak geometry have essentially confirmed the stability except for the low frequency, toroidicity induced mode which does not have its counterpart in the slab geometry. Hesketh [4] has applied the general formulation developed by Connor, Hastie and Taylor [5] for low frequency waves in tokamak geometry to the problem of electrostatic drift waves. He has found unstable solutions with $\omega \simeq \omega_{*e}$ at long perpendicular wavelength, $k_\perp \rho_i \ll 1$, with ρ_i the ion Larmor radius.

As was pointed out recently [6], the earlier studies on low frequency electrostatic modes in the tokamak geometry were based on the following ion density perturbation:

$$\frac{n_i}{n_o} = \left[\frac{\omega_{*e}}{\omega} - \frac{\omega_{De}}{\omega}\left(1 + \frac{\omega_{*i}}{\omega}\right) + \left(1 + \frac{\omega_{*i}}{\omega}\right)\left(\frac{k_\parallel^2 c_s^2}{\omega^2} - k_\perp^2 \rho_s^2\right)\right] \frac{e\phi}{T_e} \qquad (1)$$

which is not consistent with the fluid result. Here, ω_{*e} (ω_{*i}) is the electron (ion) diamagnetic frequency, both positive, ω_{De} is the electron magnetic drift frequency due to the curvature and gradient of the toroidal magnetic field, $c_s = \sqrt{T_e/M}$ is the ion acoustic speed, and $\rho_s = c_s/\Omega_i$ is the ion Larmor radius with the electron temperature. The difficulties associated with the above expression for the ion perturbation are at least twofold. In the high frequency ($\omega \gg k_\parallel c_s$), long wavelength ($k_\perp^2 \rho_s^2 \ll 1$) limits, the electrostatic dispersion relation

$$1 = \frac{\omega_{*e}}{\omega} - \frac{\omega_{De}}{\omega}\left(1 + \frac{\omega_{*i}}{\omega}\right) \qquad (2)$$

which obtains after equating the ion density to the electron density, $n_e = n_0 e\phi/T_e$, predicts a hydrodynamic instability as long as $\omega_D > 0.17\,\omega_*$, or the inverse aspect ratio $\epsilon > 0.09$, when $T_i = T_e$. (Note that, to order of magnitude, $\omega_D \simeq 2\epsilon\omega_*$.) The inequality $\epsilon > 0.09$ is satisfied by most tokamaks, and it is difficult to believe that tokamaks are subject to such a flute-like, hydrodynamic instability. Another (probably more serious) difficulty is that the electromagnetic dispersion relation [7] based on Eq. (2)

$$(\omega - \omega_*)[\omega(\omega + \omega_*) + \gamma_{MHD}^2] = k_\parallel^2 V_A^2 \left(1 + \frac{\omega_*}{\omega}\right)(\omega k_\perp^2 \rho^2 + \omega_D) \qquad (3)$$

predicts no threshold in the poloidal beta β_p for ballooning instability which becomes unstable at arbitrarily small β_p as soom as the finiteness in ω_* (finite ion Larmor radius) is introduced. Here, γ_{MHD} is the growth rate of the ideal MHD ballooning instability symbolically given by

$$\gamma_{MHD}^2 = 2\omega_*\omega_D/k_\perp^2\rho^2 - k_\parallel^2 V_A^2 \qquad (4)$$

when $T_i = T_e$, which is also assumed in Eq. (3), and $k_\parallel V_A$ is the Alfvén frequency.